Silicon composite ink for advanced photovoltaic generation prepared by low-cost technique

Supanut Laohawiroj[a], Apirak Mangkornkaew[a], Atthaphon Maneedaeng[b], and Thipwan Fangsuwannarak[a*]

[a] School of Electrical Engineering,
[b] School of Chemical Engineering, Suranaree University of Technology,
Nakhon Ratchasima, Thailand
[*]**Corresponding author**: thipwan@g.sut.ac.th

Abstract

This work describes the preparation process of crystalline silicon composite ink (Si ink) from waste silicon wafers as raw material through a grinding technique. Crystalline Si powders were homogeneously distributed in sol-gel solution via an ultrasonic shaker. The thin films of silicon dots bound with phosphorus silicate glass were produced from Si ink under drying at low-temperature by a low-cost technique as a screen printing. Micro-crystalline (μc) Si particle sizes and surface morphology of Si dots film were imaged by laser size analyzer and scanning electron microscopy, respectively. In this paper, these μc-Si dots films coating on quartz substrates were characterized by X-ray diffractometer and micro Raman spectroscopy techniques which are non-destructive optical tools to study micro- and nano-structural properties. XRD analysis revealed that ~80nm crystalline Si size in the films with relative intensity at (111) plane of 60-64% simultaneously exists into the films during the preparation at 100-400°C sintering condition. Meanwhile, the obtained Raman spectroscopy results suggest that residue stress mainly effects to the Raman asymmetric peak strongly down shifted rather than dominated by (< 10 nm) small size effect.

Keywords: *Silicon ink, silicon quantum dots, wider band gap, and tandem silicon photovoltaic.*

1. Introduction

A multi-band gap approach for an increased efficiency of tandem PV cells usually involve the use of quantum confinement in Si quantum dots (SiQDs). The decrease of nanocrystalline silicon (nc-Si) particle size affects to energy band gap enlarging for nc-Si quantum confinement of carrier leading to stronger light absorber due to quasi-direct band gap behavior [1]. The previous researches demonstrated confined energy levels of 1.7 eV for 2 nm diameter QDs embedded into its oxide matrix to be the optimum energy for an upper tandem cell element [2-3]. However, SiQDs preparation processes are almost based on high vacuum and high temperature (1000°C) procedure steps and there are also application limitations due to properties change of c-Si p/n junction at high temperature and low light absorption. In the last few decades, extensive work has been carried out on the means, which involved low-temperature and -cost process optimization and Si ink fabrication [4-5].

Synthesizes of Si nanocrystals at low temperature less than 1000 °C with high reaction yield, high quality, and high synthetic reproducibility have been investigated intensively in order to achieve significant blueshift of bandgap absorption and photoemission with enhanced energy conversion efficiency [6-7]. Nonetheless, there are no reports considerable to being concerned about synthesis of nc-Si film at low-temperature and high yield with low-cost technique using waste-silicon wafers. We foresee that a massive scale of decadent Si solar cells, which will become economic and environmental

problems will be potentially reused for applying in the third-generation solar cell. Thus, this study approaches Si wafers reusability with transmogrifying their structure into Si microstructure.

In this work, the simple production process of Si powder and fabrication procedure of Si composite ink are described. Microcrystalline Si (μc-Si) particles were bound together with silica to form the crucial part of Si dots thin films by using a screen printing technique. Furthermore, these crystalline Si properties of films were characterized by X-ray diffraction (XRD), micro Raman spectroscopy, and scanning electron microscope (SEM) techniques in order to obtain more insights of knowledge in qualitative nanocrystalline Si under low annealing temperature conditions.

2. Experimental Details

2.1. Preparation of Si powder and phosphorus silicate glass (PSG)sol-gel

Crystalline silicon (c-Si) wafers as a raw material were transmogrified through a grinding technique. Subsequently, the prepared Si powder in ethanol solution was sieved to ensure that the small Si particle sizes was obtained. The Si particle suspension formed fine Si powder after being dried at 100°C to evaporate a the volatile substance. Fine Si powders were sieved once again to ensure the uniformity of fine Si powders. Particle size distribution of μc-Si powder was verified by laser diffraction method performed by Horiba LA-950 model.

Phosphorus silicate glass (PSG) sol-gel as a binder material was prepared for functionality of Si dots matrix element, which is composed of tetra ethyl orthosilicate (TEOS, $Si(OC_2H_5)_4$, 98%), ethanol (EtOH, C_2H_5OH), othophosphoric acid (H_3PO_4, 85%) hexadecyltrimethylammonium bromide (CTAB, $C_{19}H_{42}BrN$), ethelene glycol (EG, $C_2H_6O_2$), alpha-terpineol (TP, $C_{10}H_8O$, 97%), and ethyl cellulose (EC, C_2H_5O, 48%). Firstly, TEOS and EtOH were mixed by a volume ratio of 5:1. The TEOS mixture was stirred at 70°C for 30 minutes after that H_3PO_4 was added in prepared TEOS mixture by a volume ratio (TEOS mixture: H_3PO_4) of 7:1 then the solution mixture was stirred for 30 minutes to allow well mixing. Finally, CTAB that was dissolved in EG to achieve 0.5% weight. It was dropped slowly in the solution mixture and the solution was then stirred for 30 minutes to ensure homogeneity of complete PSG sol-gel. The process steps were are shown in Figure 1

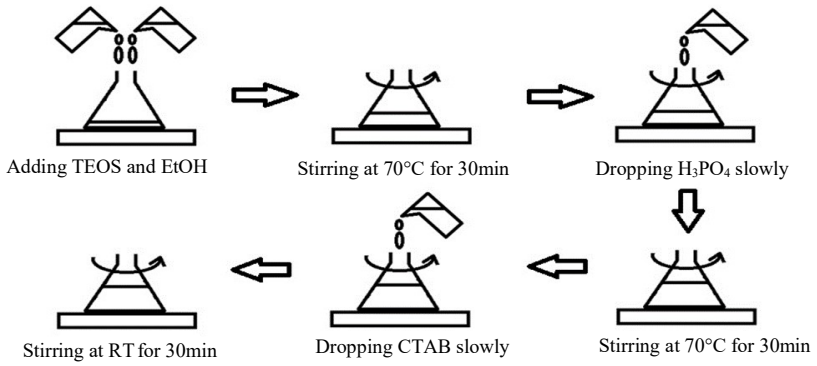

Figure 1 Procedures for preparing PSG solution

2.2. Preparation of silicon composite ink and μc-Si composite films

An organic solution consisting of terpineol (TP) and ethyl cellulose (EC) was mixed in Si-powder in a volume ratio of 1:0.22:0.28 and it was solvent by baking at 100°C for 20 minutes. PSG was dropped in

the mixed solution and shacked by ultrasonic to obtain homogenous silicon composite ink. Si ink as a crucial part that composed of micro-Si particles and phosphorus silicate sol-gel was coated on quartz substrate by screen printing technique. The μc-Si composite film was annealed at various low temperatures (100°C, 200°C, 400°C and 600°C) in air and oxygen ambient conditions for 30 minutes. The obtained films consisting of μc-Si particle enclosed with PSG were denoted as "Si dots film". For example, the samples sintered at 200°C in air and oxygen ambient conditions were denoted as "200_A Si dots" and "200_O Si dots", respectively. It is expected that the higher temperature is prone to O-Si surface oxidation and related to surface passivation due to the presence of oxygen. Oxidation at the surface of the Si nanocrystals can create surface localized states which may facilitate energy absorption and recombination processes [8].

The qualitative determination of crystallinity approximated nanocrystal is characterized by X-ray diffraction technique. XRD measurements were carried out with Cu x-ray source with the wavelength of 1.5418Å performed by a XRD D-8 Advance Bruker. Coupled two theta/theta scan type was used in order to verify both the surface and inside the film. 2 theta was scanned between 20° and 80° at 0.02° steps and 0.2 second per step. In nanocluster study, the Bragg peaks from XRD pattern are broadened due to a diffracting crystallographically coherent region becomes spatially smaller. The full width at half maximum (FWHM) value B of a Bragg peak in a 2θ scale is related to the crystallite volume size of the diffracting region (d) through the Scherrer's formula: [9-10]

$$d = \frac{k\lambda}{B\cos(\theta_B)} \quad (1)$$

where d is an average crystallite size, k is a Scherrer's constant given by 0.9, λ is a wavelength of x-ray of 1.5418 Å, B is a full width half maximum (FWHM) value of the preferential orientation peak and θ_B is the position of significant plane.

The Raman scattering experiments were carried out using Dispersive Raman Microscope (SENTERRA, Bruker) with integrating mode. An excitation source at 532 nm wavelength was used at normal incidence of laser power at 5 mW for minimizing sample heating. The resolution was 5 cm^{-1}.

3. Results and Discussion

The μc-Si powder transmogrified in this work has yields up to 80%. As observed in Figure 2, it is found that at 50% undersize the large amounts of particles obtained the average size of 4 μm as corresponding to the peak amount of each size by volume known as Q. This simple technique is very

(a)

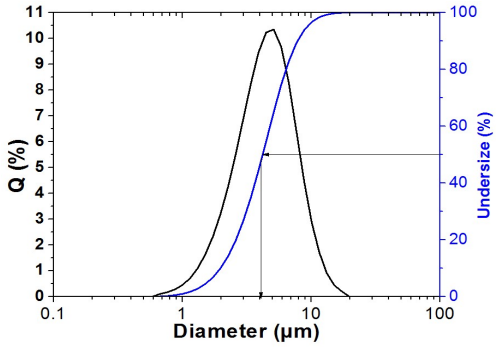

(b)

Figure 2 (a) Si powder and (b) particle size analysis of c-Si powder

cost effective to produce μc-Si powder while other expensive techniques have been used through high-temperature thermal processing [11], non-thermal plasma [12] or laser pyrolysis [13]. Si nanocrystals obtained under all complex means and high temperature procedures (1000°C) have been found to have compatibility problems with industrial manufacture.

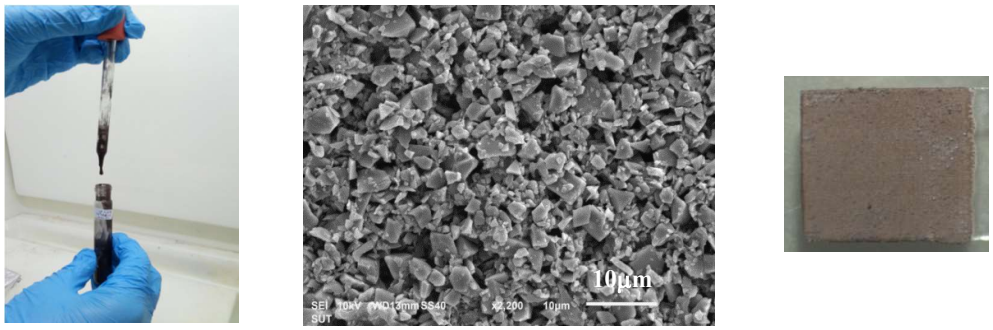

(a) (b) (c)

Figure 3 (a) Product of Si composite ink, (b) SEM image of the surface morphology of as prepared Si dots film after drying at 100°C and (c) fine Si dots thin film on a quartz

Figure 3 (a) and (b) show Si composite ink and a SEM image of the surface morphology of Si dots thin film after sintering, respectively. Surface roughness and average Si particle size of 4 μm are observed from SEM image. At this stage the Si dots thin film coated on quartz substrate are not peeling off as shown in Figure 3 (c) due to TP and EC components used for improving high adhesion of the film.

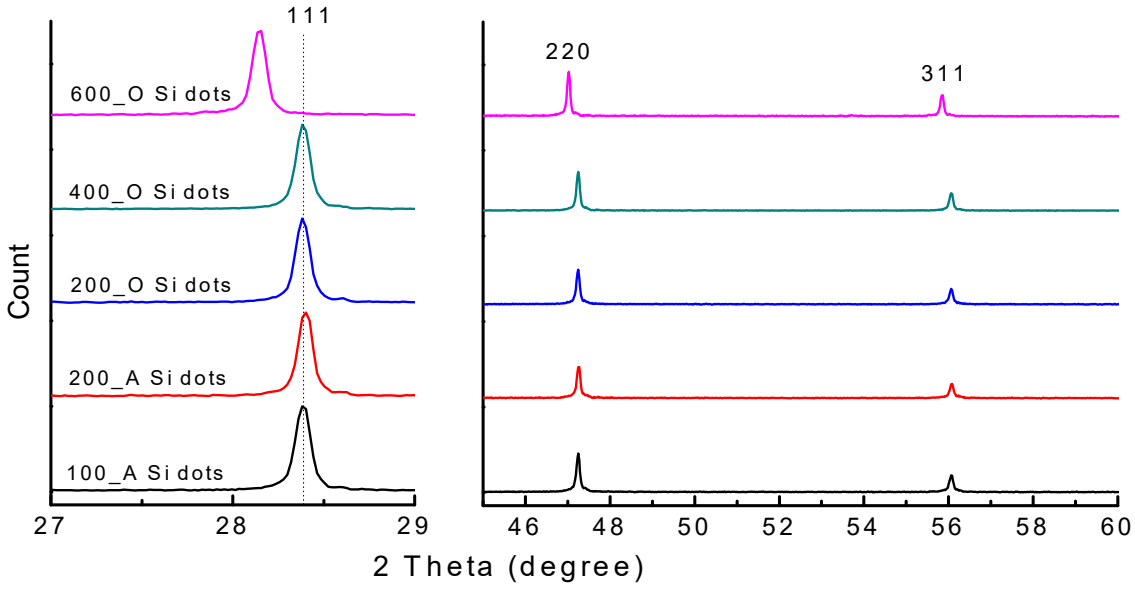

Figure 4 XRD patterns of Si dots films for study of annealing temperature dependence

In figure 4 all data shows three peaks are broadening and very close to 2θ = 28.3°, 47.1° and 56.0° corresponding to (111), (220) and (311) planes of c-Si, respectively. It is due to a decrease in the crystallite size causes an increase in the width of the diffraction [14]. Therefore, nanocrystalline Si in the thin films

under low annealing temperatures are presented in this work. The small additional peaks at 2θ = 47.1° (220) and 56.0° (311) can be connected with some metastable Si states. All XRD patterns show the strongest growth orientation along (111) to prove that the films consist of nanocrystalline Si with preferential (111) orientation. The XRD peaks represent the (111) crystallographic planes of the simple cubic structures of Si. The crystallite average size of Si dots films was evaluated by considering the highest (111) plane.

The crystallite sizes and related parameters were calculated from Scherrer's equation which uses the significant peaks of (111) planes as listed in Table 1. The results are revealed that 200_A and 200_O Si ink samples prepared under air and oxygen at 200°C show the similarity of the XRD pattern. The difference of ambient annealing conditions is independent with the average crystallite size of 85 nm. Meanwhile, as observed in SEM image the average size of granulated Si powder is around 4 μm due to the aggregates of small particles.

Table 1. Parameters calculated by XRD data

Condition	FWHM (°)	2θ (°)	Crystallite size (nm)	$d_{h,k,l}$ (Å)	a (Å)	Relative intensity % = $I_{hkl}/(I_{(111)}+I_{(220)}+I_{(311)})$		
						(111)	(220)	(311)
100_A Si-dots	0.100	28.382	81.94	3.145	5.447	60.1	27.6	12.2
200_A Si-dots	0.096	28.402	85.36	3.142	5.443	64.6	24.1	11.4
200_O Si-dots	0.096	28.382	85.36	3.145	5.447	62.4	25.8	11.8
400_O Si-dots	0.094	28.382	87.17	3.145	5.447	60.0	27.4	12.6
600_O Si-dots	0.093	28.137	88.06	3.171	5.493	55.8	29.8	14.4

The higher annealing temperature from 200°C to 600°C in oxygen ambient has an effect to a gradual increase in average crystallite size from 85.36 nm to 88.06 nm as shown in Table 1. This is possibly due to increasing agglomeration of various small nanocrystal with 600°C annealing temperature. Nevertheless, for 600_O Si dots sample annealed at 600°C the (111) peak largely shifts from 28.4° (JCPDS 00-027-1402 card of c-Si bulk) relating to a more expansion of lattice constant (a = 5.493 Å) and leading to lower (111) relative intensity of 55.8%. This shift (111) peak is most possibly related to Si cluster uniformly stained in tension and the stretching of Si-Si bonds [15]. The XRD results in this work revealed that Si dots films can be formed under low temperature preparation (100-400°C) by using Si composite ink and obtained average crystallite size in the range of 82-88 nm with high (111) relative intensity above 60%. Accordingly, the synthesis of Si dots films in order to gain high-yield at low temperature process can be developed toward the large-scale engineering production of nanocrystals and scalable process [16,17]. Thus, Si dots films achieved by powder grinding technique can approach for application in a new solar cell generation owing to low temperature preparation (100-400°C) and low-cost technique.

Figure 5 shows the Raman spectra of Si dots films for study of annealing temperature dependence on local atomic arrangements through bond frequencies and lattice-vibration (phonon) frequencies of Si-Si bond. It is found that all samples have no indication of Raman frequency spectrum with a broad hump at around 480 cm^{-1} corresponding to amorphous silicon (a-Si) portion. Meanwhile, the shape line relating to the main first-order Raman peak (Transverse optical, TO mode) around 520 cm^{-1} is found to indicate crystalline silicon (c-Si) portion. The Raman asymmetric peak to down shift from ~520 cm^{-1} to ~507 cm^{-1} with some tailing toward lower frequencies is observed. The peak asymmetry has been

assigned by some authors to a reduced phonon correlation length, related to small or defective crystalline domains [2,18-19]. However, this result closely corresponds to 2 effects: firstly, "finite size effect" of crystallite size < 10 nm due to localization of phonons in nanocrystals results in uncertainty in the phonon momentum [7, 18-19]. Secondly, "residue stress effect" is due to the lattice change of Raman frequency which is very sensitive to mechanical stress [20-21]. On the contrary, around 80 nm of crystallite size from XRD estimation will not attribute a phenomenological phonon confinement leading to "finite size effect" due to our samples exhibiting large grains. We point out that this result of the down shift of Raman asymmetric peak is most likely to take into account "residue stress effect" in Si dots enclosed with PSG. This work highlights the effect of lattice stress in the Si dots films on Raman frequency shift according to the following equation:

$$\sigma(\text{MPa}) = -250\Delta\omega(\text{cm}^{-1}) \quad (2)$$

where phonon frequency shift $\Delta\omega = \omega_s - \omega_o$, ω_s is the wave number of the stressed sample and ω_o is the wave number of the stress free single crystal. The calculation results are in rather good agreement with those measured by profilometry, assuming an error of about 10% in the case of Paillard V. work [20].

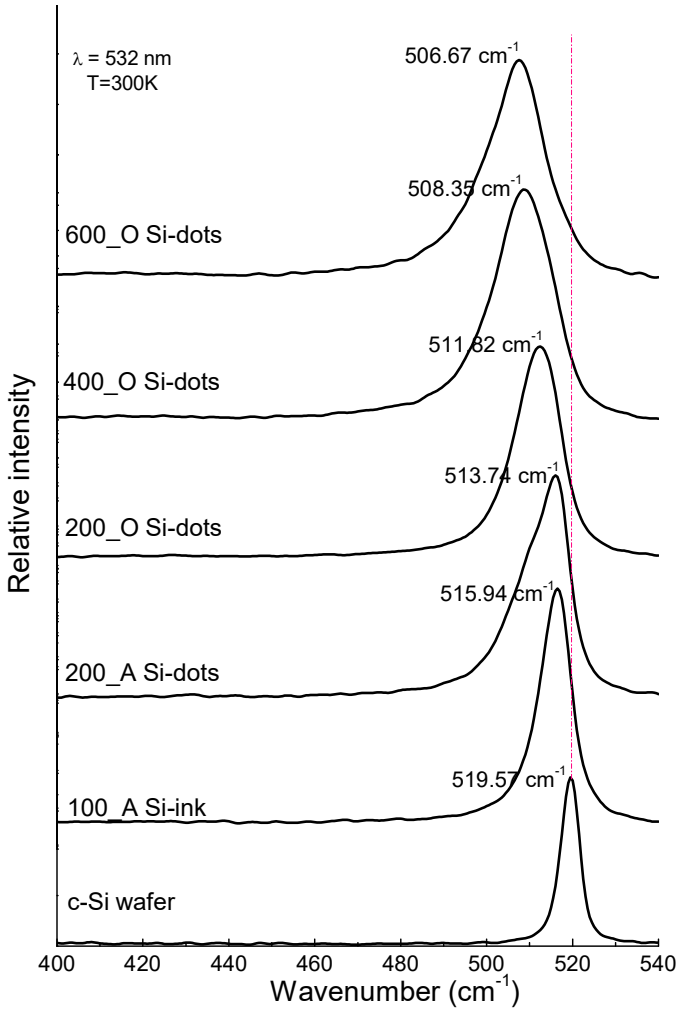

Figure 5 Raman spectra of Si dots thin films with varying temperature annealed

In Figure 6, the result suggests that an increase in annealing temperature results in an increased peak shift and implies an increased residual stress. Oxygen ambient attributes the more peak shift to the increased stress in 200O_Si dots compared with 200A_Si dots in ambient air. The temperature-dependence has agreement with increased down shift of Raman peak for Si nanowire study [22].

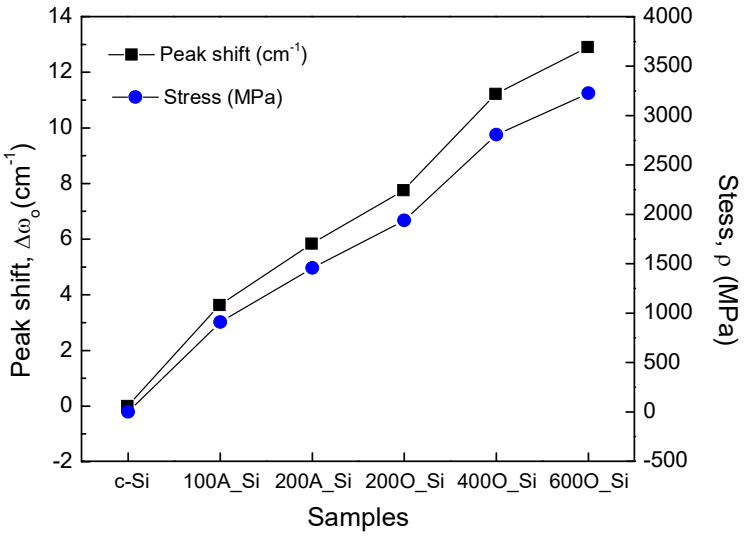

Figure 6. Annealing temperature dependence on Raman peak shift and residue stress of Si dots films

In this hypothesis, stress contribution to the Raman line shift in Si dots films would be more dominant than phonon confinement from small crystalline domain due to all Si dots films obtaining large grains (~80nm).

4. Conclusion

We have prepared Si composite ink in house) from waste silicon wafers as a main resource for producing Si dots thin film by a screen printing method. In our samples, we observed strong XRD peak of 3 main planes as-prepared sample dried at 100°C and prepared at higher annealing temperature at 600°C in O_2 ambient. The results from Raman peaks and XRD patterns indicate that the films consist of ~80 nm crystalline Si grains. Meanwhile the Raman asymmetric peak strongly down shifted corresponding to stress induced wave number shift of TO mode peak rather than be dominated by (< 10 nm) small size effect. The result suggests that higher temperature annealing results in the increased residual stress. At low temperature, ambient oxygen attributes the more peak shift to the increased stress comparing with Si dots annealed in ambient air. We conclude that Si composite ink is able to be a candidate for new nanomaterial with low-cost technique by using low temperature preparation to form Si dots film for further nanostructural solar cells.

Acknowledgements

This study was supported by Suranaree University of Technology and grant in 2018 from National Research Council of Thailand. The author would like to give gratitude to Solartron Public Company Limited Thailand and Synchrotron Light Research Institute, Thailand for equipment support.

References

[1] Green M.A.. (2003). Third generation photovoltaics: Advanced solar electricity generation. Springer Verlag, Berlin.

[2] Conibeer G., Green M.A., Cho E.C, König D., Cho Y.H., Fangsuwannarak T., Scardera G., Pink E., Huang Y., Puzzer T., Huang S., Song D., Flynn C., Park S., Hao X, Mansfield D.. (2008). Silicon quantum dot nanostructures for tandem photovoltaic cells. *Thin Solid Films*, 516., 20 6748–6756.

[3] Kintz H., Paquez X., Sublemontier O., Leconte Y., BoimeN., Reynaud C. (2015). Synthesis and layering of Si quantum dots/SiO2 composite films for third generation solar cells. *Thin Solid Film*, 593., 96-101.

[4] Sahu B.B, Yin Y., Lee J.S., Han J.G, Shiratani M. (2016). Plasma diagnostic approach for the low-temperature deposition of silicon quantum dots using dual frequency PECVD. J. Phys. D: *Appl. Phys.*, 49., 395203-395217.

[5] Antoniadis, H. (2009). Silicon ink high efficiency solar cells. 34th IEEE Photovoltaic Specialists Conference (PVSC), 650-654.

[6] J. Ouyang, Schuurmans C., Zhang Y., Nagelkerke R., Wu X., Kingston D., Wang Z.Y., Wilkinson D., Li C., Leek D.M., Tao Y., and Yu K. (2011). Low-Temperature Approach to High-Yield and Reproducible Syntheses of High- Quality Small- Sized PbSe Colloidal Nanocrystals for Photovoltaic Applications. *Appl. Mater. Interfaces*, 3., 553–565.

[7] Liu T.Y, Li M., Ouyang J., Zaman B., Wang R., Wu X., Yeh C.H., Lin Q., Yang B., and Yu K. (2009). Non-Injection and Low-Temperature Approach to Colloidal Photoluminescent PbS Nanocrystals with Narrow Bandwidth. *J. Phys. Chem.*, 113., 2301–2308.

[8] Wolkin, M., Jorne, J., Fauchet, P., Allan, G. & Delerue, C. (1999). Electronic states and luminescence in porous silicon quantum dots: the role of oxygen. *Phys. Rev. Lett*, 82., 197–200.

[9] Lin C.Y., Fang Y.K., Chen S.F., Chang S.H., Chou T.H.(2006). Enhancing photoluminescence of nanocrystalline silicon thin film with oxygen plasma oxidation. *Mater. Sci. Eng*, 134., 99.

[10] Morales M., Leconte Y., Rizk R., Chateigner D.(2004). Anisotropic crystallite size analysis of textured nanocrystalline silicon thin films probed by X-ray diffraction. *Thin Solid films*, 450., 216.

[11] Marinins A., Yang Z., Chen H., Linnros J., Veinot Jonathan G. C., Popov S., and Sychugov I. (2016). Photostable Polymer/Si Nanocrystal Bulk Hybrids with Tunable Photoluminescence. *ACS Photonics*, 3., 1575-1580.

[12] Xiaodong P., Qing L., Dongsheng L. and Deren Y.(2011). Spin-coating silicon-quantum-dot ink to improve solar cell efficiency. *Solar Energy Materials & Solar Cells*, 95., 2941–2945.

[13] Kintz H., Paquez X., Sublemontier O., Leconte Y., Nathalie H-B. and Reynaud C. (2015). Synthesis and layering of Si quantum dots/SiO2 composite films for third generation solar cells. *Thin Solid Films*, 593., 96–101.

[14] Camden R. Hubbard. (1982). Standard reference material 640a silicon powder 2θ/d-Spacing Standard for X-ray Diffraction. USA: Washington, D.C., 20234.

[15] Comedi D., Zalloum O.H.Y,Irving E.A, Wojcik J., Roschuk T. Flynn M.J, and Mascher P. (2006). X-ray-diffraction study of crystalline Si nanocluster formation in annealed silicon-rich silicon oxides. *Journal of Applied Physics*, 99., 235181-235188

[16] Campbell I.H., and Fauchet P.M.(1986). The effects of microcrystal size and shape on the one phonon Raman spectra of crystalline semiconductors. *Solid State Communications*, 58., 739.

[17] Jian Zi, H. Büscher, C. Falter, W. Ludwig, Kaiming Zhange and Xide Xie. (1996). Raman shifts in Si nanocrystals. *Appl. Phys. Lett.*, 69., 200

[18] Richter H., Wang Z. P., and Ley L. (1981). The one phonon Raman spectrum in microcrystalline silicon. *Solid State Communications*, 39., 625-629.

[19] Mishra P. and Jain K. P. (2001). First- and second-order Raman scattering in nanocrystalline silicon. *Phys, Rev*, 64., 073304.

[20] Paillard V., Puech P., Laguna M.A., Temple-Boyer P., Caussat B., Coudere J.P., and de Mauduit B.(1998). Resonant Raman scattering in polycrystalline silicon thin films. *Appl. Phys. Lett*., 73., 1718.

[21] Arguirov T., Mchedlidze T., Kittler M., Rölver R., Berghoff B., Först M., and Spangenberg B.(2006). Residual stress in Si nanocrystals embedded in a SiO2SiO2 matrix. *Appl. Phys. Lett.*, 89., 053111.

[22] Zixue S., Jian S., Guowei P., Jianxun L., Deren Y., Calum D. and Wuzong Z. (2006). Temperature-Dependent Raman Scattering of Silicon Nanowires. *J. Phys. Chem. B.*, 110., 1229-1234.